J Immunotoxicol, 2014; 11(4): 359–366

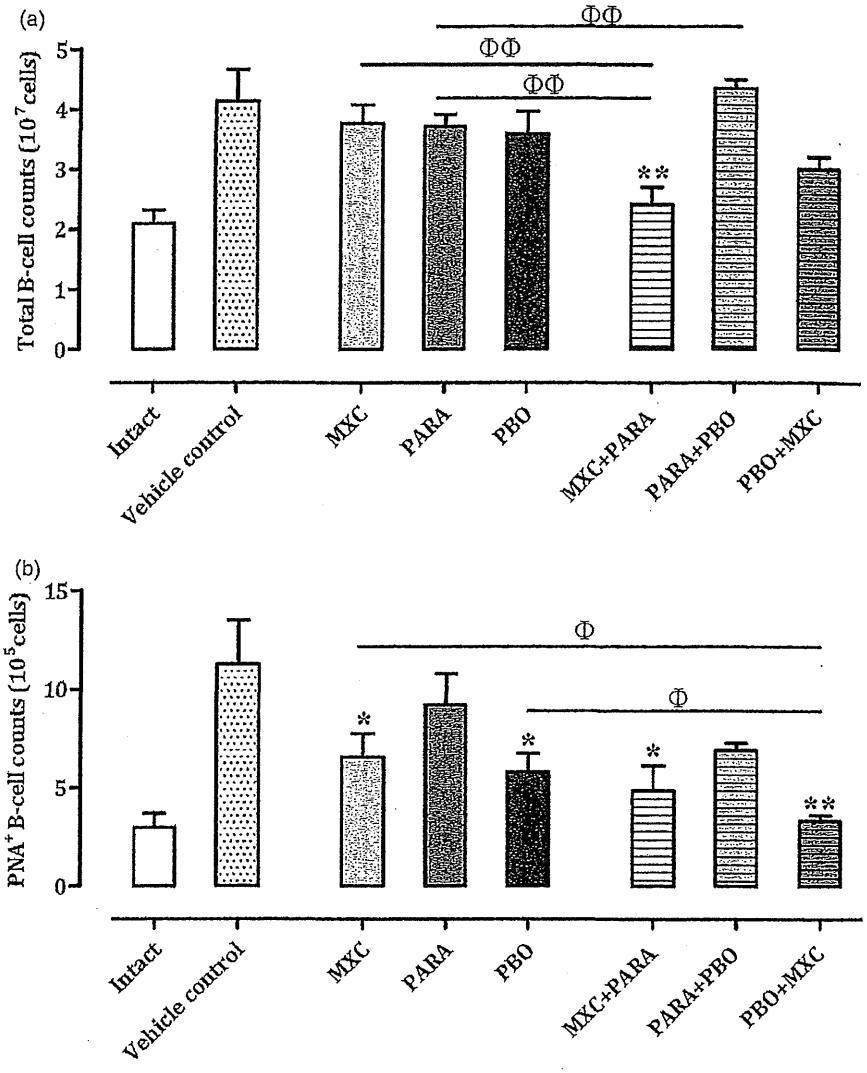

Figure 4. Total B-cell and germinal center B-cell counts in spleens. Mice were treated as described in the Figure 1 legend. (a) Total B-cell and (b) germinal center B-cell counts are shown. Results for intact, vehicle, and individual agent-treated mice are included in each chart. Cell counts are expressed as mean ± SD ($n = 8$ per group). $^*p < 0.05$ and $^{**}p < 0.01$ (Dunnett's multiple comparison test) vs vehicle control group; $\Phi p < 0.05$ and $\Phi\Phi p < 0.01$ (Student's t-test) vs single test substance groups.

from their individual agent counterparts. These results suggested to us that, at the level of thymocyte damage (i.e. potential apoptosis), there was little to no interactive effect from the combined exposures to PARA + PBO and PBO + MXC exposures. In contrast, as MXC + PARA exposure appeared to have induced a more severe effect compared with exposure to each individual chemical, it is likely that some interactive effect (most likely synergistic) was occurring *in situ* to amplify the toxicities of each individual test agent. As will become clear below, this *preferentially* strong toxicity by MXC + PARA compared to the other combinational regimens becomes evident in several other aspects of these studies.

SRBC is a common antigen used to evaluate general immune status. After immunization with SRBC, SRBC-specific IgM responses in serum and spleen can be assessed using ELISA and PFC assays, respectively (Temple et al., 1993; White et al., 2010). Use of these two assays allows for evaluation of the mechanisms of action of xenobiotic-induced immunotoxicities (Herzyk & Holsapple, 2007). Compared with the vehicle control mice, MXC + PARA and PBO + MXC mice had significant decreases in serum SRBC-specific IgM responses, whereas MXC, PARA, PBO, and PARA + PBO mice did not. In addition, the IgM responses with the MXC + PARA mice were significantly decreased vs that of MXC mice, and PBO + MXC treatment led to significant decreases relative to those seen with PBO and MXC mice. In contrast, in all groups given a test substance, spleen SRBC-specific IgM PFC responses were significantly decreased relative to those seen with the vehicle control group. In addition, the SRBC-specific IgM responses with spleens from the PBO + MXC mice were significantly decreased compared to that of organs from PBO mice. Based on our historic data (Fukuyama et al., 2013), the peak response to SRBC for the SRBC-specific IgM ELISA occurs ~2 days after the maxima that would be used to optimize results for a PFC. Thus, as we utilized a protocol that was focusing mainly on the PFC assay, it is not a complete surprise that the SRBC-specific IgM ELISA responses were weaker than the PFC ones. Under these conditions, MXC + PARA and PBO + MXC led to significant decreases relative to those seen with PBO and MXC in serum SRBC-specific IgM responses. These results suggested to us that MXC + PARA or PBO + MXC exposures induced a more severe reduction in humoral immune responses compared with exposure to any of the three individual chemicals.

To further clarify mechanisms of MXC + PARA- or PBO + MXC-induced immunosuppression, total, helper, and cytotoxic T-cell counts, as well as total and germinal center B-cell counts in the spleens were analyzed via flow cytometry based on cell-specific surface makers (Janeway et al., 2004). It was clear that the MXC + PARA combined treatment damaged T-cells. Total, helper, and cytotoxic T-cell counts in hosts that received this combined treatment were decreased compared with those in vehicle control, MXC, and PARA mice. In contrast,

in the PBO + MXC hosts, the counts were comparable to those in PBO- and MXC-only mice. Similarly, in PARA + PBO mice, all sets of counts were comparable to those in PARA and PBO mice. These latter sets of results indicated that the toxicities of these two chemical combinations, at least in regard to impacts on T-cell populations *in situ*, were similar to those of any of their single chemical constituents. It is interesting to note that, with the MXC + PARA regimen, the changes in cell counts corresponded with the observed changes in SRBC-specific IgM responses. On the other hand, in the PBO + MXC group, although SRBC-specific IgM responses were decreased compared to the control, PBO, and MXC mice, there were no similar correspondence with the T-cell measures. This might suggest that the combined action of the PBO and MXC may have been directed more against the B-cell aspects of humoral responses than against T-cells; however, this still remains to be verified in more detailed studies.

In an immune response, local activated B-cells act as antigen-presenting cells for helper or cytotoxic T-cells (Goutet et al., 2005), proliferate, and differentiate into plasma cells to secrete antigen-specific antibodies. Some B-cells are activated at the T/B-cell border and migrate to form germinal centers (in primary follicles; Janeway et al., 2004); therefore, changes in the numbers of germinal centers and associated B-cells can reflect major responses to exposure to antigens or toxicants (Vieira & Rajewsky, 1990; Takahashi et al., 1998). A marked decrease in total B-cell counts was seen in the MXC + PARA-treated mice compared with that in MXC and PARA mice. Neither other combinational treatment had a similar significant effect. At the germinal center level, both MXC + PARA and PBO + MXC led to significant reductions in B-cell levels; PARA + PBO had no significant impact. Compared to their individual agents, MXC + PARA treatment caused even greater reductions in total B-cell levels, but had no effect at the germinal center level. This contrasts with PBO + MXC that had the opposite effect, i.e. no impact at total B-cell level but significantly-so at germinal centers. While these opposing outcomes are without explanation at this point, the upshot is that the combinational treatments with PBO + MXC or MXC + PARA are toxic to B-cells *in situ*. Toxicity from PARA + PBO is nominal at best.

The findings with the PBO + MXC mice supports our contention cited in the early paragraphs about potentially more selective effects on B-cells. That the MXC + PARA regimen also impacted on B-cells (beyond above-noted effects on thymic weights, T-cell counts, and IgM responses) suggested that this specific combination displayed a far more immunotoxic targeting than the other combined regimen. Whether such a divergent effect is due to differences in synergizing effects from each individual agent is an interesting possibility. Future studies with gradational combinations of each test chemical should allow us to ascertain which of the individual agents is driving any synergisms.

Conclusions

Our data show that combined exposure to certain environmental chemicals can induce immunotoxicity, as shown by effects on SRBC-specific IgM responses and T- or B-cell counts, compared to that by individual exposure to the chemicals in mixtures. However, this toxicity appears to differ, depending on which chemicals are combined. In particular, it was clear that, among the three combinations, MXC + PARA presented the most immunotoxic profile in the murine hosts. The combined toxicity may be affected by chemical structure, receptor binding, and immune pathways involved; further studies are currently in progress. It is expected that the results of this study will help others in their evaluation of immunotoxic combinational effects when conducting assessments of the safety of environmental/occupational chemicals.

Acknowledgements

This work was supported by a research Grant-in-Aid from the Ministry of Health, Labor, and Welfare of Japan. The authors wish to thank Mrs Y. Tajima and L. Miyashita of the Institute of Environmental Toxicology (Ibaraki, Japan) for their technical assistance.

Declaration of interest

The authors report no conflicts of interest. The authors alone are responsible for the content and writing of the paper.

References

Battaglia, C. L., Gogal Jr., R. M., Zimmerman, K., and Misra, H. P. 2010. Malathion, lindane, and piperonyl butoxide, individually or in combined mixtures, induce immune-toxicity via apoptosis in murine splenocytes *in vitro*. *Int. J. Toxicol.* 29:209–220.

Casale, G. P., Cohen, S. D., and DiCapua, R. A. 1984. Parathion-induced suppression of humoral immunity in inbred mice. *Toxicol. Lett.* 23: 239–247.

Committee on Proprietary Medicinal Products. 2000. *Note for Guidance on Repeat-Dose Toxicity*, CPMP/SWP/1042/99. Available online at: http://www.emea.eu.int.

Cunningham, A. J. 1965. A method of increased sensitivity for detecting single antibody-forming cells. *Nature* 207:1106–1107.

Diel, F., Horr, B., Borck, H., et al. 1999. Pyrethroids and piperonyl-butoxide affect human T-lymphocytes *in vitro*. *Toxicol. Lett.* 107: 65–74.

EPA (United States Environmental Protection Agency). 1998. *Health Effects Test Guidelines: Immunotoxicity*. 1998, OPPTS 870.7800. Available online at: http://www.epa.gov/opptsfrs/publications

FDA (United States Food and Drug Administration). 2002. *Guidance for Industry: Immuotoxicology Evaluation of Investigational New Drugs*. Available online at: http://www.fda.gov/cder/guidance

Feron, V. J., Groten, J. P., Jonker, D., et al. 1995. Toxicology of chemical mixtures: Challenges for today and the future. *Toxicology* 105: 415–427.

Flipo, D., Bernier, J., Girard, D., et al. 1992. Combined effects of selected insecticides on humoral immune response in mice. *Int. J. Immunopharmacol.* 14:747–752.

Fukuyama, T., Kosaka, T., Hayashi, K., et al. 2013. Immunotoxicity in mice induced by short-term exposure to methoxychlor, parathion, or piperonyl butoxide. *J. Immunotoxicol.* 10:150–159.

Fukuyama, T., Tajima, Y., Ueda, H., and Kosaka, T. 2011. Prior exposure to immunosuppressive organophosphorus or organochlorine compounds aggravates the T(H)1- and T(H)2-type allergy caused by topical sensitization to 2,4-dinitrochlorobenzene and trimellitic anhydride. *J. Immunotoxicol.* 8:170–182.

Fukuyama, T., Tajima, Y., Ueda, H., et al. 2010. Apoptosis in immunocytes induced by several types of pesticides. *J. Immunotoxicol.* 7:39–56.

Gilbert, K. M., Rowley, B., Gomez-Acevedo, H., and Blossom, S. J. 2011. Co-exposure to mercury increases immunotoxicity of trichloroethylene. *Toxicol. Sci.* 119:281–292.

Goutet, M., Pepin, E., Langonne, I., et al. 2005. Identification of contact and respiratory sensitizers using flow cytometry. *Toxicol. Appl. Pharmacol.* 205:259–270.

Groten, J. P., Feron, V. J., and Suhnel, J. 2001. Toxicology of simple and complex mixtures. *Trends. Pharmacol. Sci.* 22:316–322.

Groten, J. P., Schoen, E. D., van Bladeren, P. J., et al. 1997. Subacute toxicity of a mixture of nine chemicals in rats: Detecting interactive effects with a fractionated two-level factorial design. *Fundam. Appl. Toxicol.* 36:15–29.

Hernandez, A. F., Parron, T., Tsatsakis, A. M., et al. 2013. Toxic effects of pesticide mixtures at a molecular level: Their relevance to human health. *Toxicology* 307:136–145.

Herzyk, D. J., and Holsapple, M. 2007. Immunotoxicity evaluation by immune function tests: Focus on the T-dependent antibody response (TDAR). Overview of Workshop Session at 45th Annual Meeting of Society of Toxicology March 5-9, 2006 San Diego, CA. *J. Immunotoxicol.* 4:143–147.

Holsapple, M. P. 2003. Developmental immunotoxicity testing: A review. *Toxicology* 185:193–203.

ICH. 2006. International Conference on harmonization of technical requirements for registration of pharmaceuticals for human use. *ICH Harmonized Tripartite Guideline Immunotoxicity Studies For Human Pharmaceuticals S8*. Switzerland: ICH.

Institoris, L., Papp, A., Siroki, O., et al. 2002. Immuno- and neurotoxicological investigation of combined subacute exposure with the carbamate pesticide propoxur and cadmium in rats. *Toxicology* 178:161–173.

Institoris, L., Siroki, O., Undeger, U., et al. 1999. Immunotoxicological effects of repeated combined exposure by cypermethrin and the heavy metals lead and cadmium in rats. *Int. J. Immunopharmacol.* 21:735–743.

Janeway, C. A., Travers, P., Walport, M., and Shlomchik, M. J., (Eds.). 2004. *Immunobiology*, 6th Edition. New York: Grand Science.

Jerne, N. K., and Nordin, A. A. 1963. Plaque formation in agar by single antibody-producing cells. *Science* 140:405.

Kortenkamp, A., Faust, M., Scholze, M., and Backhaus, T. 2007. Low-level exposure to multiple chemicals: Reason for human health concerns? *Environ. Health. Perspect.* 115:106–114.

Lowry, O. H., Rosebrough, N. J., Farr, A. L., and Randall, R. J. 1951. Protein measurement with the Folin phenol reagent. *J. Biol. Chem.* 193:265–275.

Luster, M. I., Munson, A. E., Thomas, P. T., et al. 1988. Development of a testing battery to assess chemical-induced immunotoxicity: National Toxicology Program's guidelines for immunotoxicity evaluation in mice. *Fundam. Appl. Toxicol.* 10:2–19.

Mitsumori, K., Takegawa, K., Shimo, T., et al. 1996. Morphometric and immunohistochemical studies on atrophic changes in lymphohematopoietic organs of rats treated with piperonyl butoxide or subjected to dietary restriction. *Arch. Toxicol.* 70:809–814.

Nishino, R., Fukuyama, T., Tajima, Y., et al. 2013. Prior oral exposure to environmental immunosuppressive chemicals methoxychlor, parathion, or piperonyl butoxide aggravates allergic airway inflammation in NC/Nga mice. *Toxicology* 309C:1–8.

Simmons, J. E. 1995. Chemical mixtures: Challenge for toxicology and risk assessment. *Toxicology* 105:111–119.

Smialowicz, R. J., DeVito, M. J., Riddle, M. M., et al. 1997. Opposite effects of 2,2′,4,4′,5,5′-hexachlorobiphenyl and 2,3,7,8-tetrachlorodibenzo-*p*-dioxin on the antibody response to sheep erythrocytes in mice. *Fundam. Appl. Toxicol.* 37:141–149.

Takahashi, Y., Dutta, P. R., Cerasoli, D. M., and Kelsoe, G. 1998. *In situ* studies of the primary immune response to (4-hydroxy-3-nitrophenyl)-acetyl. V. Affinity maturation develops in two stages of clonal selection. *J. Exp. Med.* 187:885–895.

Takeuchi, Y., Kosaka, T., Hayashi, K., et al. 2002b. Alterations in the developing immune system of the rat after perinatal exposure to methoxychlor. *J. Toxicol. Pathol.* 17:165–170.

Takeuchi, Y., Kosaka, T., Hayashi, K., et al. 2002a. Thymic atrophy induced by methoxychlor in rat pups. *Toxicol. Lett.* 135: 199–207.

Temple, L., Kawabata, T. T., Munson, A. E., and White Jr., K. L. 1993. Comparison of ELISA and plaque-forming cell assays for measuring the humoral immune response to SRBC in rats and mice treated with benzo[a]pyrene or cyclophosphamide. *Fundam. Appl. Toxicol.* 21: 412–419.

Teuschler, L., Klaunig, J., Carney, E., et al. 2002. Support of science-based decisions concerning the evaluation of the toxicology of mixtures: A new beginning. *Regul. Toxicol. Pharmacol.* 36: 34–39.

Vieira, P., and Rajewsky, K. 1990. Persistence of memory B-cells in mice deprived of T-cell help. *Int. Immunol.* 2:487–494.

White, K. L., Musgrove, D. L., and Brown, R. D. 2010. The sheep erythrocyte T-dependent antibody response (TDAR). *Meth. Mol. Biol.* 598:173–184.

Bioorganic & Medicinal Chemistry Letters 24 (2014) 2582–2584

Contents lists available at ScienceDirect

Bioorganic & Medicinal Chemistry Letters

journal homepage: www.elsevier.com/locate/bmcl

Synthesis and radical-scavenging activity of a dimethyl catechin analogue

Kohei Imai [a], Ikuo Nakanishi [b], Akiko Ohno [c], Masaaki Kurihara [c], Naoki Miyata [d], Ken-ichiro Matsumoto [b], Asao Nakamura [a], Kiyoshi Fukuhara [e,*]

[a] Department of Applied Chemistry, Shibaura Institute of Technology, Fukasaku, Minuma-ku, Saitama 337-8570, Japan
[b] Research Center for Charged Particle Therapy, National Institute of Radiological Sciences, Inage-ku, Chiba 263-8555, Japan
[c] Division of Organic Chemistry, National Institute of Health Sciences, Setagaya-ku, Tokyo 158-8501, Japan
[d] Graduate School of Pharmaceutical Sciences, Nagoya City University, Mizuho-ku, Nagoya, Aichi 467-8603, Japan
[e] School of Pharmacy, Showa University, Hatanodai, Shinagawa-ku, Tokyo 142-8555, Japan

ARTICLE INFO

Article history:
Received 6 January 2014
Revised 10 March 2014
Accepted 12 March 2014
Available online 20 March 2014

Keywords:
Antioxidant
Synthetic antioxidant
Catechin
Radical scavenging

ABSTRACT

Catechin analogue **1** with methyl substituents *ortho* to the catechol hydroxyl groups was synthesized to improve the antioxidant ability of (+)-catechin. The synthetic scheme involved a solid acid catalyzed Friedel–Crafts coupling of a cinnamyl alcohol derivative to 3,5-dibenzyloxyphenol followed by hydroxylation and then cyclization through an intermediate orthoester. The antioxidative radical scavenging activity of **1** against galvinoxyl radical, an oxyl radical, was found to be 28-fold more potent than (+)-catechin.

Among natural bioactive compounds distributed in fruits, vegetables, and beverages of plant origin, phenolic antioxidants (ArOH), such as flavonoids, tocopherol, and resveratrol, are widely recognized for their biological and pharmacological effects that include anti-carcinogenic, anti-cardiovascular anti-neurodegenerative, and anti-inflammatory properties.[1–4] These properties are principally attributed to the capacity of these compounds to trap reactive oxygen species and to chelate metal ions, which through the Fenton reaction could generate radicals.[5] Therefore, this so-called antioxidative ability of phenolic compounds is frequently cited as the key to their success in the prevention and/or reduction of oxidative stress-related chronic diseases and age-related disorders. Consideration of antioxidative ability in drug development has led to interest in improving the radical scavenging activity of phenolic compounds based on the antioxidant mechanism.[6] Antioxidant activity via the direct quenching of free radicals is expressed in two mechanisms: a one-step hydrogen atom transfer from the phenolic OH group to the free radical and a single-electron transfer from ArOH to the free radical with concomitant formation of the radical cation $ArOH^{\bullet+}$.[7] The former process, characterized by vitamin E, is based on the capacity of a phenol to donate a hydrogen atom to a free radical.[8] Catechin and resveratrol (see Fig. 1 for the structures) scavenge free radicals by the latter mechanism.[9,10] In this case, the ionization potential (IP) of the phenol is important for the radical scavenging efficacy. Hence, introduction of electron-donating substituents at positions *ortho* and/or *para* to the phenolic hydroxyl group would decrease the IP of ArOH, thereby enhancing the radical scavenging ability. In this regard, planar catechin analogues, in which an isopropyl fragment as electron-donor was introduced into (+)-catechin by reaction with acetone, exhibited 5-fold more potent radical scavenging activity than (+)-catechin.[11] An epigallocatechin analogue with a similarly introduced isopropyl fragment also displayed increased radical scavenging activity.[12] In the case of *ortho*-alkyl substituents, the $ArOH^{\bullet+}$ formed in the reaction with a free radical is stabilized by compensation of the electron vacancy by either an inductive effect or through hyperconjugation, resulting in improved radical scavenging ability. Resveratrol analogues with one and two methyl groups at positions *ortho* to the phenol hydroxyl group showed 14- and 36-fold acceleration in the ability to scavenge free radicals, respectively.[13]

The aim of the present study was to synthesize the catechin analogue **1** in which both positions *ortho* to the catechol hydroxyl groups were substituted with methyl groups. Compared with (+)-catechin, the dimethyl analogue of catechin showed greatly enhanced radical scavenging ability against galvinoxyl radical as a model radical for reactive oxygen species. This result indicates

* Corresponding author. Tel.: +81 3 3784 8186; fax: +81 3 3784 8252.
E-mail address: fukuhara@pharm.showa-u.ac.jp (K. Fukuhara).

http://dx.doi.org/10.1016/j.bmcl.2014.03.029
0960-894X/

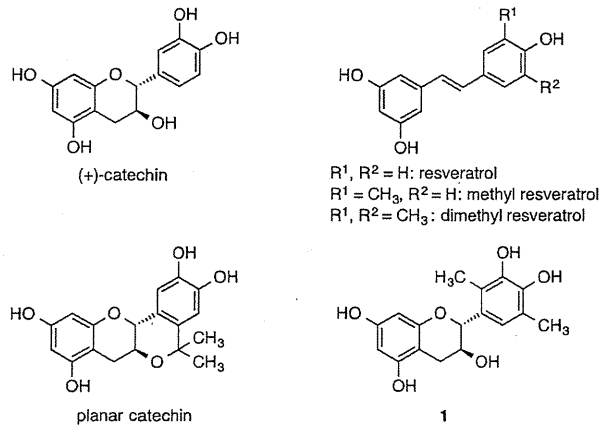

Figure 1. Structures of catechin, resveratrol, and their analogues.

there is a role for the antioxidant chemistry of phenols via a radical scavenging mechanism that is accelerated by electron-donating substituents.

There are numerous methods for construction of the flavonoid skeleton using a biomimetic strategy.[14,15] The synthetic strategy employed here is an efficient and general approach to access the flavan framework of **1**. This process consisted of a solid acid catalyzed Friedel–Crafts coupling of cinnamyl alcohol derivative **2**, that included an embedded dimethylcatechol moiety, with 3,5-dibenzyloxyphenol **3**, followed by hydroxylation and cyclization to give the corresponding dimethyl catechin derivative.

The synthesis of **2** is outlined in Scheme 1. Introduction of methyl groups at both *ortho* positions of the catechol could be readily accomplished by Mannich reaction of catechol using morpholine and formamide to afford **4**. Palladium catalyzed hydrogenation of **4** was carried out with heating at 70 °C under a high pressure of hydrogen gas to give dimethylcatechol **5**. Since **5** was highly sensitive, the subsequent reactions, formylation with $CH(OEt)_3$ followed by benzyl protection of the hydroxyl groups of catechol **6**, were performed using the crude reaction products. The resulting compound **7** was subjected to Knoevenagel condensation with monoethyl malonate in pyridine containing a catalytic amount of piperidine to produce α,β-unsaturated ester **8**. Reduction of **8** with LAH/$AlCl_3$ gave the corresponding cinnamyl alcohol **2**.

Phenol **3**, obtained by the method of Lehmann and Jahr,[16] was subjected to Friedel–Crafts alkylation with **2** using H_2SO_4/SiO_2 as catalyst in CS_2/CH_2Cl_2 to furnish the coupled product **9** as shown in Scheme 2. Oxidation of **9** with NMO in the presence of a catalytic amount of OsO_4 gave the *cis*-diol product **10**, which was converted into *ortho*-ester **11** with triethyl orthoformate and a catalytic amount of pyridinium *p*-toluenesulfonate (PPTS) at room temperature. The reaction was continued with heating at 60 °C to form the flavan framework as intermediate formate ester **12**. De-esterification of **12** with K_2CO_3 in 1,2-dimethoxyethane/methanol and debenzylation using $Pd(OH)_2$ and H_2 in THF/methanol afforded **1** (Fig. 1).

The radical scavenging activity of **1** was evaluated in a non-aqueous system using galvinoxyl radical (GO·) as an oxyl radical species. Because of its odd electron, GO· exhibits a strong absorption band at 428 nm, and a solution of GO· appears yellow in color. As the electron is paired, the absorption vanishes, and the resulting decolorization is stoichiometric with respect to the number of electrons taken up. Taking advantage of the color change of GO· in the presence of an antioxidant, the rate of radical scavenging of **1** toward galvinoxyl was measured. As shown in Figure 2, the decay rate of the absorbance at 428 nm followed pseudo first-order kinetics when the concentration of **1** was maintained at more than 10-fold excess to the GO· concentration. The pseudo first-order rate constant (k_{obs}) exhibited first-order dependence with respect to the concentration of **1** as shown in Figure 3. From the linear plot of k_{obs} versus [**1**], the second-order rate constant (k) for the radical scavenging of **1** toward GO· was determined to be 1.07×10^3 $mol^{-1}\,dm^3\,s^{-1}$. The k value for (+)-catechin was determined in the

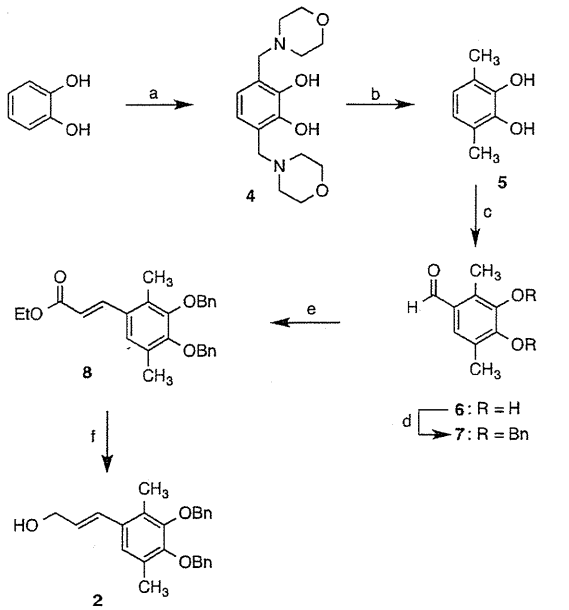

Scheme 1. Reagents and conditions: (a) morpholine, formaldehyde, EtOH, rt, 61%; (b) H_2, 10% Pd/C, THF, 5 atm, 70 °C; (c) $CH(OEt)_3$, $AlCl_3$, toluene, rt; (d) BnBr, K_2CO_3, KI, acetone, rt, 3.2% (total yield from **4**); (e) monoethyl malonate, piperidine, pyridine, reflux, 87%; (f) LAH, $AlCl_3$, THF, rt, 48%.

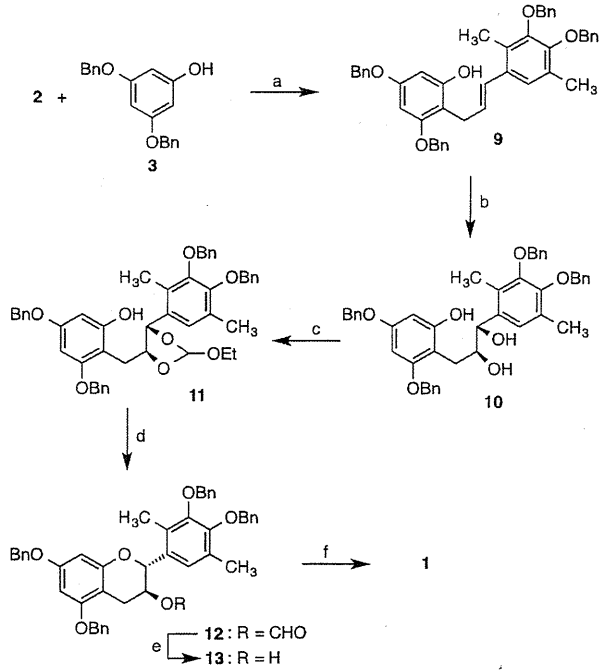

Scheme 2. Reagents and conditions: (a) H_2SO_4/SiO_2, CH_2Cl_2, rt, (b) NMO, OsO_4, acetone, H_2O, rt, 37% (total yield from **2**); (c) $CH(OEt)_3$, PPTS, EDC, rt; (d) $CH(OEt)_3$, PPTS, EDC, 60 °C; (e) K_2CO_3, MeOH, DMF, rt, 89% (a total yield from **10**); (f) H_2, $Pd(OH)_2$, MeOH, THF, rt, 56%.

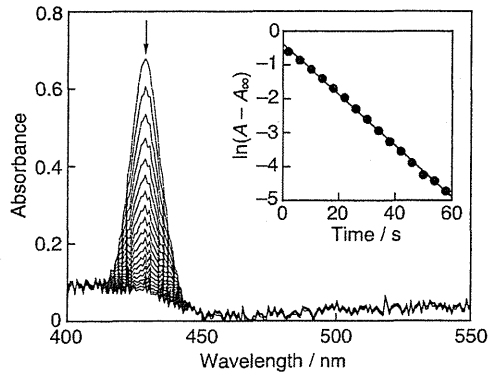

Figure 2. Spectral changes observed during the reaction between dimethyl catechin analogue **1** (6.8×10^{-5} mol dm^{-3}) and GO· (4.7×10^{-6} mol dm^{-3}) in deaerated MeCN at 298 K (interval: 2 s). Inset: first-order plot based on the decay of the absorption at 428 nm for GO·.

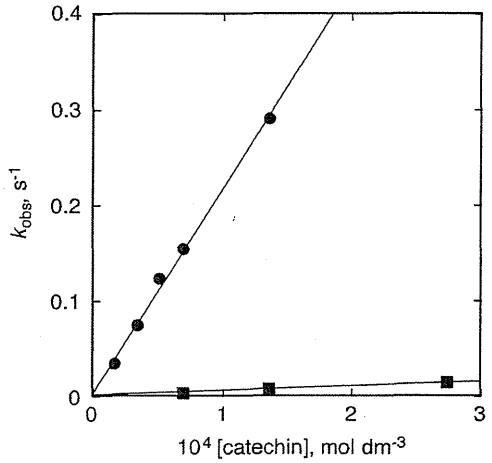

Figure 3. Plot of the pseudo first-order rate constants (k_{obs}) versus the concentrations of **1** and (+)-catechin for the radical scavenging reaction toward GO·.

same manner to be 3.87×10 mol^{-1} dm^3 s^{-1}. These results indicate that the introduction of methyl groups at both positions *ortho* to the catechol hydroxyl groups led to a 28-fold increase in radical scavenging activity.

In conclusion, the dimethyl analogue of catechin, **1**, was synthesized to demonstrate a strategy to enhance radical scavenging ability that may aid in the prevention and therapy of various oxidative stress related diseases. Indeed, the scavenging rate constant of GO· by **1** was greatly increased as compared to catechin. Since inductive and hyperconjugation effects of methyl groups can contribute to stabilization of the radical cation of catechol formed in the reaction with GO·, the enhanced radical scavenging activity of **1** supports the antioxidant chemistry of catechin occurring by the scavenging of oxyl free radicals through a single electron transfer mechanism. This simple derivatization by methyl substituents makes it possible to improve the radical scavenging activity of catechin without causing a fatal change in the overall structure that may be significantly associated with its inherent biological activities, and this strategy is likely to be of value in medicinal chemistry applications.

Supplementary data

Supplementary data associated with this article can be found, in the online version, at http://dx.doi.org/10.1016/j.bmcl.2014.03.029.

References and notes

1. Gonzalez-Vallinas, M.; Gonzalez-Castejon, M.; Rodriguez-Casado, A.; Ramirez de Molina, A. *Nutr. Rev.* **2013**, *71*, 585.
2. Aggarwal, B. B.; Sundaram, C.; Prasad, S.; Kannappan, R. *Biochem. Pharmacol.* **2010**, *80*, 1613.
3. Arranz, S.; Chiva-Blanch, G.; Valderas-Martinez, P.; Medina-Remon, A.; Lamuela-Raventos, R. M.; Estruch, R. *Nutrients* **2012**, *4*, 759.
4. Albarracin, S. L.; Stab, B.; Casas, Z.; Sutachan, J. J.; Samudio, I.; Gonzalez, J.; Gonzalo, L.; Capani, F.; Morales, L.; Barreto, G. E. *Nutr. Neurosci.* **2012**, *15*, 1.
5. Heim, K. E.; Tagliaferro, A. R.; Bobilya, D. J. *J. Nutr. Biochem.* **2002**, *13*, 572.
6. Bansal, S.; Vyas, S.; Bhattacharya, S.; Sharma, M. *Nat. Prod. Rep.* **2013**, *30*, 1438.
7. Quideau, S.; Deffieux, D.; Douat-Casassus, C.; Pouysegu, L. *Angew. Chem., Int. Ed.* **2011**, *50*, 586.
8. Nakanishi, I.; Fukuhara, K.; Shimada, T.; Ohkubo, K.; Iizuka, Y.; Inami, K.; Mochizuki, M.; Urano, S.; Itoh, S.; Miyata, N.; Fukuzumi, S. *J. Chem. Soc., Perkin Trans. 2* **2002**, 1520.
9. Nakanishi, I.; Miyazaki, K.; Shimada, T.; Ohkubo, K.; Urano, S.; Ikota, N.; Ozawa, T.; Fukuzumi, S.; Fukuhara, K. *J. Phys. Chem. A* **2002**, *106*, 11123.
10. Nakanishi, I.; Shimada, T.; Ohkubo, K.; Manda, S.; Shimizu, T.; Urano, S.; Okuda, H.; Miyata, N.; Ozawa, T.; Anzai, K.; Fukuzumi, S.; Ikota, N.; Fukuhara, K. *Chem. Lett.* **2007**, *36*, 1276.
11. Fukuhara, K.; Nakanishi, I.; Kansui, H.; Sugiyama, E.; Kimura, M.; Shimada, T.; Urano, S.; Yamaguchi, K.; Miyata, N. *J. Am. Chem. Soc.* **2002**, *124*, 5952.
12. Imai, K.; Nakanishi, I.; Anzai, K.; Ozawa, T.; Miyata, N.; Urano, S.; Okuda, H.; Nakamura, A.; Fukuhara, K. *Chem. Lett.* **2011**, *40*, 1417.
13. Fukuhara, K.; Nakanishi, I.; Matsuoka, A.; Matsumura, T.; Honda, S.; Hayashi, M.; Ozawa, T.; Miyata, N.; Saito, S.; Ikota, N.; Okuda, H. *Chem. Res. Toxicol.* **2008**, *21*, 282.
14. Nay, B.; Collet, M.; Lebon, M.; Cheze, C.; Vercauteren, J. *Tetrahedron Lett.* **2002**, *43*, 2675.
15. Bianco, A.; Cavarischia, C.; Farina, A.; Guiso, M.; Marra, C. *Tetrahedron Lett.* **2003**, *44*, 9107.
16. Lehmann, M.; Jahr, M. *Org. Lett.* **2006**, *8*, 721.

PLOS | ONE

RESEARCH ARTICLE

The 4′-Hydroxyl Group of Resveratrol Is Functionally Important for Direct Activation of PPARα

Yoshie Takizawa[1], Rieko Nakata[1], Kiyoshi Fukuhara[2], Hiroshi Yamashita[3], Hideo Kubodera[3], Hiroyasu Inoue[1]*

1 Department of Food Science & Nutrition, Nara Women's University, Nara, Japan, **2** Showa University School of Pharmacy, Tokyo, Japan, **3** Medicinal Chemistry Research Laboratories, Mitsubishi Tanabe Pharma Corporation, Kanagawa, Japan

* inoue@cc.nara-wu.ac.jp

OPEN ACCESS

Citation: Takizawa Y, Nakata R, Fukuhara K, Yamashita H, Kubodera H, Inoue H (2015) The 4′-Hydroxyl Group of Resveratrol Is Functionally Important for Direct Activation of PPARα. PLoS ONE 10(3): e0120865. doi:10.1371/journal.pone.0120865

Academic Editor: Anindita Das, Virginia Commonwealth University, UNITED STATES

Received: September 13, 2014

Accepted: January 27, 2015

Published: March 23, 2015

Data Availability Statement: All relevant data are within the paper.

Funding: This work was supported by Grants-in-Aid for Scientific Research (Nos. 19300250 and 24300217 to H.I. and R.N.) from the Ministry of Education, Culture, Sports, Science, and Technology of Japan; the Iijima Memorial Foundations for the Promotion of Food Science and Technology; Uehara Memorial Foundation of Nutrition; and the Japan Food Chemical Research Foundation. The funders had no role in study design, data collection and analysis, decision to publish, or preparation of the manuscript.

Abstract

Long-term moderate consumption of red wine is associated with a reduced risk of developing lifestyle-related diseases such as cardiovascular disease and cancer. Therefore, resveratrol, a constituent of grapes and various other plants, has attracted substantial interest. This study focused on one molecular target of resveratrol, the peroxisome proliferator activated receptor α (PPARα). Our previous study in mice showed that resveratrol-mediated protection of the brain against stroke requires activation of PPARα; however, the molecular mechanisms involved in this process remain unknown. Here, we evaluated the chemical basis of the resveratrol-mediated activation of PPARα by performing a docking mode simulation and examining the structure-activity relationships of various polyphenols. The results of experiments using the crystal structure of the PPARα ligand-binding domain and an analysis of the activation of PPARα by a resveratrol analog 4-phenylazophenol (4-PAP) *in vivo* indicate that the 4′-hydroxyl group of resveratrol is critical for the direct activation of PPARα. Activation of PPARα by 5 μM resveratrol was enhanced by rolipram, an inhibitor of phosphodiesterase (PDE) and forskolin, an activator of adenylate cyclase. We also found that resveratrol has a higher PDE inhibitory activity (IC_{50} = 19 μM) than resveratrol analogs trans-4-hydroxystilbene and 4-PAP (IC_{50} = 27-28 μM), both of which has only 4′-hydroxyl group, indicating that this 4′-hydroxyl group of resveratrol is not sufficient for the inhibition of PDE. This result is consistent with that 10 μM resveratrol has a higher agonistic activity of PPARα than these analogs, suggesting that there is a feedforward activation loop of PPARα by resveratrol, which may be involved in the long-term effects of resveratrol *in vivo*.

Introduction

The phytoalexin resveratrol (3, 5, 4′-trihydroxystilbene) [1] possesses antioxidant properties and has multiple effects, including the inhibition or suppression of cyclooxygenase (COX)

Competing Interests: All authors have declared that no competing interests exist in this revised manuscript. Two of the authors are employed by a commercial company, Medicinal Chemistry Research Laboratories, Mitsubishi Tanabe Pharma Corporation, Kanagawa, Japan. This does not alter the authors' adherence to PLOS ONE policies on sharing data and materials.

[2], [3], and the activation of peroxisome proliferator activated receptors (PPARs) [4] and the NAD^+-dependent protein deacetylase sirtuin 1 (SIRT1) [5]. Previous studies show that resveratrol can prevent or slow the progression of various cancers, cardiovascular diseases, and ischemic injuries, as well as enhancing stress resistance and extending life-span [6], [7].

Resveratrol is a calorie-restriction mimetic [8] with potential anti-aging and anti-diabetogenic properties; therefore, its ability to activate SIRT1 has attracted particular interest. However, the activation of SIRT1 by resveratrol *in vitro* appears to be an artifact generated by the use of fluorophore-tagged substrates [9], [10]. A recent study reported that cAMP-dependent phosphodiesterase (PDE) is a direct target of resveratrol and suggested that the metabolic effects of the compound are mediated by PDE inhibition [11]; however, this proposal remains unconfirmed. Previous studies by our group focused on the hypothesis that the beneficial effects of resveratrol require the direct activation of PPARα [4], [12], [13], which is supported by reports that PPARα mediates some of the effects of calorie restriction [14].

PPARs are members of a nuclear receptor family of ligand-dependent transcription factors [15]. The three PPAR isoforms, PPARα (NR1C1), β/δ (NR1C2), and γ (NR1C3), show distinct tissue distributions and play various roles in lipid and carbohydrate metabolism, cell proliferation and differentiation, and inflammation, and are considered molecular targets for the treatment of lifestyle-related diseases [15], [16]. The ligand-binding domains of the PPAR isoforms share 60–70% sequence identity, although all three isoforms bind naturally occurring fatty acids [17]. The prostaglandin D_2-derived metabolite, 15-deoxy-$\Delta^{12,14}$- prostaglandin J_2, is a potent natural ligand of PPARγ [18], [19]. We previously reported that this metabolite suppresses lipopolysaccharide-induced expression of COX-2, a key inflammatory enzyme in prostaglandin synthesis, in macrophage-like U937 cells but not in vascular endothelial cells [20]. We also demonstrated that the expression of COX-2 is regulated by negative feedback mediated by PPARγ, especially in macrophages [20]. These findings indicate that PPARs participate in the cell type-specific control of COX-2 expression [3], which led us to hypothesize that resveratrol is a direct activator of PPARs. This proposal is supported by the results of *in vitro* reporter assays in bovine arterial endothelial cells (BAECs) [21], which demonstrated that 5 μM resveratrol activates PPARα, β/δ, and γ [4], [13]. In a study using PPARα-knockout mice, resveratrol treatment (20 mg/kg weight/day for 3 days) protected the brain against ischemic injury through a PPARα-dependent mechanism, indicating that resveratrol activates PPARα *in vivo* [4]. Moreover, we also demonstrated that the resveratrol tetramer, vaticanol C, activates PPARα and PPARβ/δ both *in vitro* (5 μM) and *in vivo* (0.04% of the diet for 8 weeks), although no effects on SIRT1 were observed [13].

In light of the findings described above, the aim of this study was to evaluate the chemical basis of the activation of PPARα by resveratrol.

Materials and Methods

Reagents and cell culture

Resveratrol was purchased from Sigma and the other plant polyphenols were purchased from Wako Chemicals (Japan). Azobenzene and 4-phenylazophenol (4-PAP) were purchased from Tokyo Chemicals, and trans-4-hydroxystilbene (T4HS) was synthesized as reported previously [22]. A 100 mM stock solution of each compound was prepared in DMSO and the stock was diluted to the working concentration before use. BAECs (Cell Applications, San Diego, CA) were grown in DMEM supplemented with 10% fetal calf serum.

Transcription assays and construction of mutated PPARα expression vectors

BAECs were transfected with 0.15 μg of the tk-PPREx3-Luc reporter plasmid, 0.15 μg of the human PPARα expression vector pGS-hPPARα (GeneStorm clone L02932; Invitrogen), and 0.04 μg of the pSV-βgal vector, using Trans IT-LT-1 (Mirus) as described previously [20], [23]. Twenty-eight hours after transfection, the BAECs were incubated with the relevant chemical for 24 h, after which the cells were harvested and lysed, and luciferase and β-galactosidase activities were measured. The luciferase activities were normalized to those of the β-galactosidase standard. The validity of this reporter assay was previously confirmed using Wy-14643, GW501516, and pioglitazone, which are synthetic agonists of PPARα, β/δ, and γ, respectively [23]. Site-directed mutagenesis of PPARα to form I241A, L247A, F273A, I317A and I354A was performed using an inverse PCR method, the KOD-Plus-Mutagenesis Kit (Toyobo, Japan), pGS-hPPARα as a template, and mutagenic primers. Mutagenic primers used were: F273A 5′- gctcactgctgccagtgcacgtcagtggagaccgtcac-3′ (forword), 5′- gatgcggacctccgccaccaagttcaggatgccattgg-3′ (reverse); I354A 5′- gccatggaacccaagtttgattttgc catgaagttcaat-3′ (forword), 5′- atcacagaacggtttccttaggctttttaggaattcacg-3′ (reverse); I241A 5′- gcacatgatatggagacactgtgtatg-3′ (forword), 5′- tgcgacaaaaggtggattgttactg-3′ (reverse); L247A 5′- agcatgtatggctgagaagacgctgg-3′ (forword), 5′- gccatacatgctgtctccatatcatgtatgac-3′ (reverse); I317A 5′- gcattcgccatgctgtcttctgtg-3′ (forword), 5′- tgcggcctcataaactccgtattttagc-3′ (reverse). All mutations were confirmed by DNA sequencing.

Docking mode prediction and free energy calculations

The docking modes of resveratrol were predicted using the GOLD 3.0 docking program [24]. The protein co-ordinates were taken from the PPARα-GW409544 complex structure (PDB ID: 1K7L) and the amino acid residues within 12 Å of GW409544 were assumed to be the target binding site. The docking procedure with GOLD 3.0 was repeated 150 times, and the 150 docking poses were clustered to obtain four representative poses. Molecular dynamics simulations were performed using the AMBER 8 program and the Cornell force field 94. The solvent water was the SPC model and the cubic periodic boundary condition was used. The Coulomb interaction was evaluated using the particle mesh Ewalt method. The protein-ligand complex structure was moved with a time step of 2 femtoseconds and hydrogens were constrained with the SHAKE algorithm. After standard minimization and equilibration of the protein-ligand complex, simulation was performed for 1 nanosecond and 1,000 snapshots were collected. A Molecular Mechanical/Poisson-Boltzmann Surface Area analysis [25] was performed with a standard protocol. Computational alanine scanning was performed in a similar manner to that described above, mutating each amino acid in turn.

Animal experiments

Male 8-week-old SV/129-strain (wild-type) and PPARα-knockout mice (Jackson Laboratory) were housed in a room at 24 ± 2°C with a 12 h/12 h light/dark cycle and were fed the AIN93-G diet or the same diet supplemented with 0.04% 4-PAP. Food and water were available ad libitum. After 8 weeks of feeding, the mice were anesthetized with isoflurane, and euthanized by collecting a blood sample using a syringe. Livers were removed and stored in RNA later solution (Ambion, USA) at -30°C. Body weight, food consumption and liver weight were not significantly different between 4-PAP-fed mice and control. In addition, plasma AST and ALT level of 4-PAP-fed mice were same level as control (data not shown). This study was carried out in accordance with the guideline for Care and Use of Laboratory Animals published by Minister

of the Environment Government of Japan (No. 88 of April 28, 2006). All experimental procedures were approved by the Animal Care Committee of Nara Women's University. All efforts were made to minimize suffering.

Real-time PCR

Total RNA was isolated using the acid guanidinium thiocyanate procedure. Real-time RT-PCR was performed using the Mx3005 system (Stratagene) as described previously [23]. Expression levels of each mRNA were normalized to those of GAPDH mRNA. PCR primers used were: GAPDH 5′- ggtgaaggtcggagtcaacgga-3′ (forword), 5′- gagggatctcgctcctggaaga-3′ (reverse); Acyl CoA oxidase 1 5′- gggagtgctacgggttacatg-3′ (forword), 5′- ccgatatccccaacagtgatg-3′ (reverse); Carnitine palmitoyltransferase 1A 5′- cttccatgactcggctcttc-3′ (forword), 5′- aaacagttc-cacctgctgct-3′ (reverse); Adiponectin receptor type 2 5′- acccacaaccttgcttcatc-3′ (forword), 5′- ggcagctccggtgatataga-3′ (reverse); Fatty acid binding protein 1 5′- aagtaccaattgcagagccagga-3′ (forword), 5′- ggtgaactcattgcggacca-3′ (reverse); Long-chain acyl CoA dehydrogenase 5′- cagttgcatgaaaccaaacg-3′ (forword), 5′- gacgatctgtcttgcgatca-3′ (reverse); SIRT1 5′- gtcaga-taaggaaggaaaac-3′ (forword), 5′- tggctctatgaaactgttct-3′ (reverse).

PDE inhibition assay

The PDE inhibition assay was performed using the PDE-Glo™ Phosphodiesterase assay (Promega). Bovine brain-derived PDE, majority of which was PDE4 isozyme [26], was purchased from Sigma. One milliunit of PDE was pre-incubated with varying concentrations of rolipram (Wako Chemicals, Japan), resveratrol, T4HS or 4-PAP for 30 min at room temperature, and then 1 μM cAMP substrate was added and the reactions were incubated for a further 90 minutes at 37°C. Luminescence was measured using the Tecan Infinite 200 plate-reader.

Statistical analysis

All results are expressed as the mean ± SD. Comparisons between groups were performed using unpaired *t*-tests or two-way ANOVA with post-hoc Bonferroni multiple comparison test. Values were deemed to be statistically significantly different at $p < 0.05$.

Results and Discussion

The 4′-hydroxyl group of resveratrol is required for the activation of PPARα *in vitro*

First, we investigated whether resveratrol and its related compounds (Fig. 1A) are able to activate PPARα in a cell-based luciferase reporter assay. BAECs were transiently transfected with the PPRE-luc reporter vector, the human PPARα expression vector GS-hPPARα, and pSV-β-gal as an internal control, and then incubated with 5, 10 μM resveratrol or its related compounds for 24 h. The activation of PPARα by resveratrol was suppressed by the addition of a 3′-hydroxyl group (to form piceatannol), by the replacement of the 3,5-hydroxyl groups with methoxy groups (to form pterostilbene), and by deletion of the 3,4-hydroxyl groups from resveratrol (to form T4HS) (Fig. 1A, B). The activation of PPARα by 4-PAP, which has a chemical structure similar to that of T4HS instead of the stilbene to azobenzene backbone (Fig. 1A), was similar to that by T4HS, and that, the level of activation was reduced further following deletion of the hydroxyl group (to form azobenzene) These compounds showed the dose-dependent increase of PPARα activation except for azobenzene (Fig. 1A, B).

Next, we compared the PPARα-activating ability of other polyphenols with a flavone backbone (Fig. 1C) with that of resveratrol. The compounds studied were as follows: apigenin,

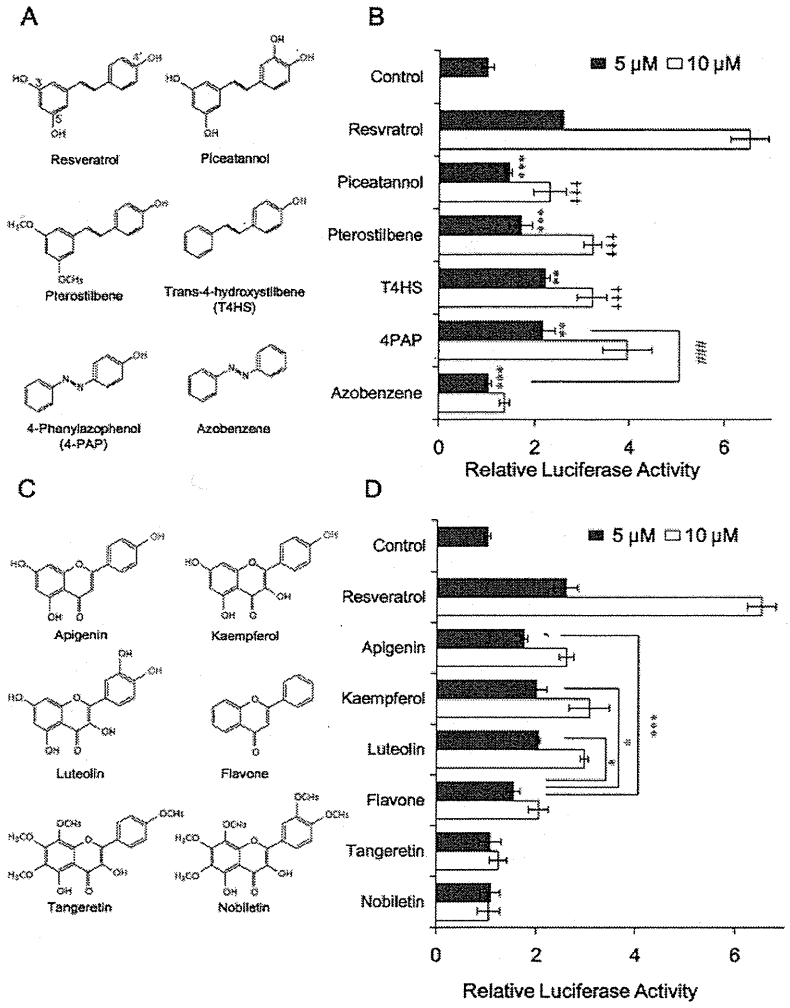

Fig 1. The 4′-hydroxyl group of resveratrol is required for the activation of PPARα *in vitro*. (A) The chemical structures of resveratrol and its related compounds containing a 4′-hydroxyl group (shown in red). (B) The activation of PPARα by exposure of BAECs transiently transfected with PPRE-luc, GS-hPPARα, and pSV-β-gal to the compounds (5, 10 μM) shown in (A). Data were statistically evaluated using the unpaired *t*-test. ** $p < 0.01$, *** $p < 0.001$ compared with cells treated with 5 μM resveratrol. ††† $p < 0.001$ compared with cells treated with 10 μM resveratrol. ### $p < 0.001$ compared with cells treated with 4-PAP. (C) The chemical structures of the flavonoids studied. (D) The activation of PPARα by exposure of BAECs transiently transfected with PPRE-luc, GS-hPPARα, and pSV-β-gal to 5 μM of resveratrol or to 5 μM of the flavonoids shown in (C). Data were statistically evaluated using the unpaired *t*-test. * $p < 0.05$, *** $p < 0.001$ compared with cells treated with flavone. (B) and (D) were presented as the relative luciferase activities normalized to those of the β-galactosidase standard, and represent the mean ± SD of three independent wells of cells. Similar results were obtained by two additional experiments.

doi:10.1371/journal.pone.0120865.g001

which has a similar 4′-hydroxyl group to that of resveratrol; kaempferol and luteolin, both of which have chemical structures similar to that of apigenin but contain an additional one or two hydroxyl groups, respectively; a flavone with no hydroxyl group; and tangeretin and nobiletin, which have four or five methoxy groups, respectively, one of which replaces the 4′-hydroxyl

group of resveratrol (Fig. 1C). The abilities of apigenin, kaempferol, and luteolin to activate PPARα were approximately 20–35% lower than that of resveratrol (Fig. 1D). The flavone that lacked hydroxyl groups displayed 55% of the activating ability of resveratrol and the ability of flavone to activate PPARα was significantly lower than that of apigenin, kaempferol and luteolin. The abilities of these compounds to activate PPARα at 10 μM were higher than 5 μM except for tangeretin and nobiletin (chemicals with no "corresponding 4'-OH"). These results indicate that the 4′-hydroxyl group of resveratrol is functionally important for the activation of PPARα although the contribution of this 4′-hydroxyl group may differ between the stilbene and flavone backbones.

Identification of a plausible docking model and identification of F273 and I354 as PPARα residues involved in resveratrol binding

The X-ray crystal structure of the PPARα LBD as a complex with its synthetic agonist GW409544 and a co-activator motif from steroid receptor co-activator 1 was reported previously [27]. The hydrogen bonds between the carboxylate of GW409544, Tyr314 on helix 5, and Tyr464 on the AF2 helix, act as a molecular switch that activates the transcriptional activity of PPARα [27]. The docking modes of resveratrol were predicted using the GOLD 3.0 docking program [24] and protein co-ordinates from the PPARα-GW409544 complex structure (PDB ID: 1K7L). Four modes were predicted; the four orientations of the nearly planar molecule are horizontal or vertical mirror images (Fig. 2A). Of the four predicted modes, modes I and II, which are vertical mirror images, seem feasible for two reasons. First, when the calculated docking mode II of resveratrol was superimposed on the PPARα-GW409544 complex structure, the configuration of resveratrol (Fig. 2B; orange) partially overlapped that of GW409544 (Fig. 2B; green). Second, the 4′-hydroxyl group of resveratrol was in the vicinity of the hydroxyl groups of Tyr314 and Tyr464, suggesting the possibility of hydrogen bond formation between them. The 3,5-hydroxyl groups of resveratrol were located near to hydrophobic amino acid residues, suggesting that they do not contribute much to the binding affinity for PPARα. This proposal is consistent with the finding that removing these groups (to form T4HS) had a slight but significant suppressive effect on the ability of resveratrol to activate PPARα (Fig. 1B). The binding features were also consistent with the experimental observation that the 4′-hydroxyl group is a crucial functional moiety for PPARα activation (Fig. 1).

In modes III and IV, which are horizontal mirror images of modes II and I, respectively, the 4′-hydroxyl group would be located further away from Tyr314 and Tyr464; therefore, these modes may not be compatible with the apparent importance of this group to PPARα activation. However, the binding free energies predicted using a Molecular Mechanical/Poisson-Boltzmann Surface Area analysis [25] showed that modes II (-10.28 ± 9.12 kcal/mol) and IV (-15.64 ± 9.31 kcal/mol) are more plausible than mode I (-1.28 ± 11.12 kcal/mol), although it is worth noting that the free energy for GW409544 binding is-35.63 ± 11.79 kcal/mol. Ideally, these calculations should be based on crystallographically determined complex co-ordinates, although we resorted to docking predictions here. Taken together, this information suggests that mode II is the most plausible docking model for resveratrol (Fig. 2C).

A computational alanine scanning technique was then used to examine the contribution of each PPARα amino acid residue around the ligand. We were predicted that the residues F273 and I354 were the most favorable sites for binding the free energy of resveratrol in mode II whereas the residues I241, L247 and I317 were not favorable sites in mode II. Consistent with these predictions, site-directed mutagenesis of either of these residues (F273A or I354A) reduced the activation of PPARα by resveratrol compared with others (I241A, L247A, and I317A) (Fig. 2D) in BAECs transiently transfected with the PPRE-luc reporter. On the other

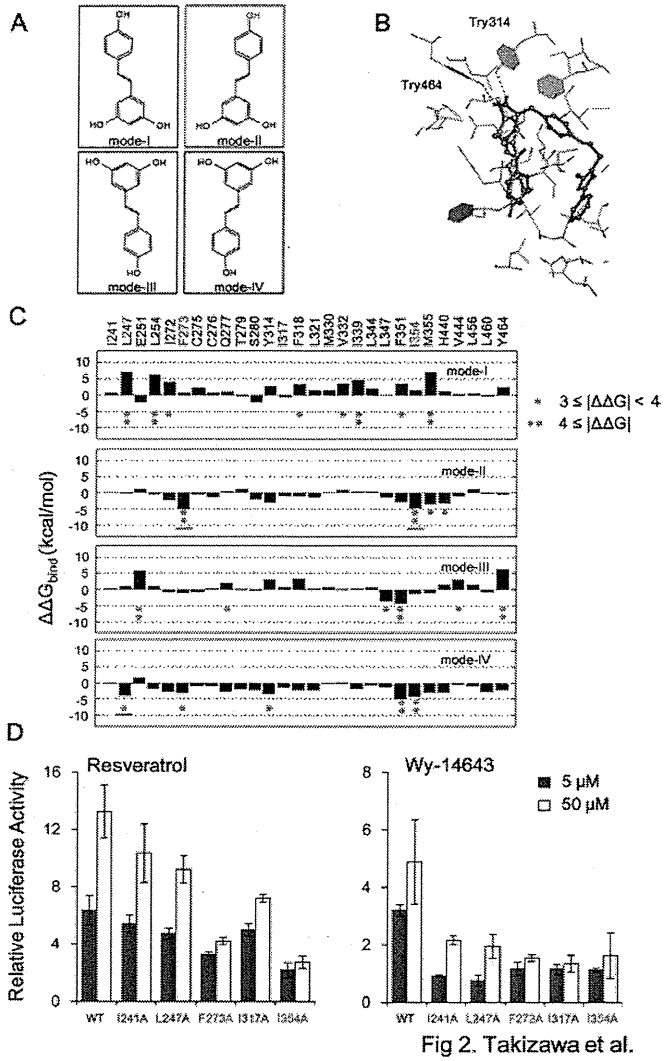

Fig 2. Takizawa et al.

Fig 2. Docking models and analysis of PPARα residues required for binding to resveratrol. (A) The four docking modes of resveratrol predicted using the GOLD 3.0 docking program [24] with protein co-ordination data from the PPARα-GW409544 complex structure (PDB ID: 1K7L) and a standard docking protocol. (B) Superimposition of docking mode II of resveratrol (orange) on the structure of PPARα bound to GW409544, a potent PPARα agonist (green). Only the amino acids located near to GW409544 are displayed. The hydrogen bonds of Tyr314 and Tyr464 are shown as dashed green lines. (C) Binding free energies (ΔΔGbind (kcal/mol)) of the indicated PPARα amino acid residues, calculated by alanine scanning using data for the four predicted docking modes. (D) Activation of wild-type (WT) PPARα and its mutants by 5, 50 μM resveratrol or Wy-14643. BAECs were transiently transfected with PPRE-luc, wild-type or mutant GS-hPPARα, and pSV-β-gal. The data are presented as relative luciferase activities normalized to those of the β-galactosidase standard and as 1 for cells treated with DMSO (control), and represent the mean ± SD of three independent wells of cells. Similar results were obtained by two additional experiments. The data were calculated the relative luciferase activity in cells transfected with wild-type PPARα.

doi:10.1371/journal.pone.0120865.g002

hand, all mutants (I241A, L247A, F273A, I317A, and I354A) were suppressed by Wy-14643. These results provide additional evidence that docking mode II of resveratrol is plausible, and that its 4′-hydroxyl group is functionally important for PPARα activation. In this study, we did not show that resveratrol directly binds to PPARα, however, our collaborated study showed

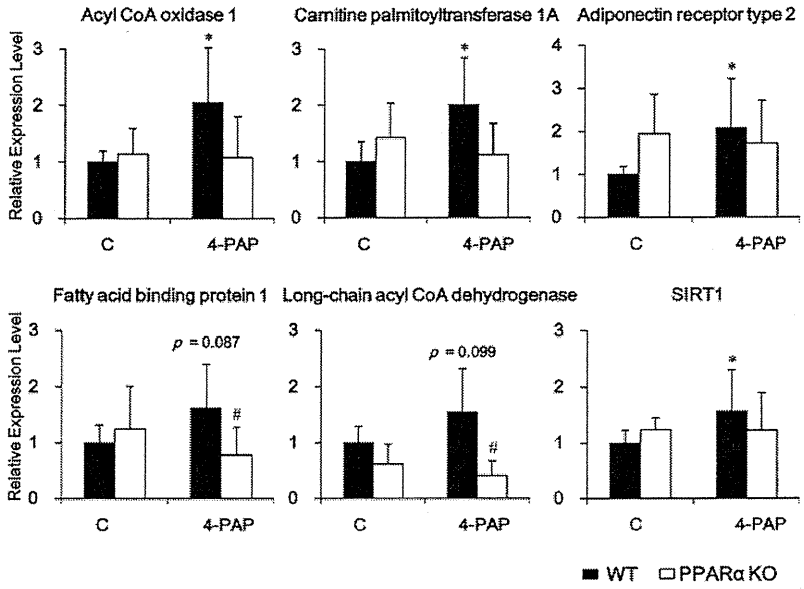

Fig 3. Takizawa et al.

Fig 3. 4-PAP induces PPARα-dependent genes and SIRT1 *in vivo*. RT-qPCR was used to determine the mRNA levels of the indicated genes in liver samples from wild-type (WT; filled columns) and PPARα-knockout (PPARα KO; open columns) mice fed the control AIN-93G diet (C) or the same diet supplemented with 0.04% 4-PAP for 8 weeks. Data represent the mean ± SD from 7–8 mice in each group (WT) and from 4 mice in each group (PPARα KO). Data were statistically evaluated using the unpaired two-way ANOVA with post-hoc Bonferroni multiple comparison test. $^{*}p < 0.05$ compared with wild-type mice fed the control diet. $^{\#}p < 0.05$ compared with wild-type mice fed the 4-PAP-supplemented diet. For each mRNA, data were normalized to the expression levels in wild-type mice fed the control diet.

doi:10.1371/journal.pone.0120865.g003

the direct interaction between resveratrol and PPARγ by X-ray crystal structure analysis (unpublished data), which is also recently reported by another group [28].

4-PAP induces the expression of PPARα-dependent genes and SIRT1

Next, the importance of the 4′-hydroxyl group of resveratrol to the activation of PPARα *in vivo* was examined. A previous study demonstrated that exposure of wild-type mice to 0.04% vaticanol C, a resveratrol tetramer, upregulates the hepatic expression of PPARα-responsive genes such as fatty acid binding protein 1. However, this response was not observed in PPARα-knockout mice, indicating that vaticanol C activates PPARα *in vivo* [13]. Similarly, we recently found that exposure of wild-type mice (but not PPARα-knockout mice) to 0.04% resveratrol for 4 weeks upregulates the hepatic expression of SIRT1 and PPAR-responsive genes such as Acyl CoA oxidase 1, Long-chain acyl CoA dehydrogenase, and Fatty acid binding protein 1 (unpublished data), indicating that resveratrol also activates PPARα *in vivo*. Here, a resveratrol analog 4-PAP, which has a 4′-hydroxyl group on an azobenzene backbone (Fig. 1A), was used to examine the importance of this group to the activation of PPARα *in vivo*. Compared with wild-type mice fed a control diet, those exposed to 0.04% 4-PAP for 8 weeks showed significantly higher hepatic expression levels of the PPARα-responsive genes such as Acyl CoA oxidase 1, Carnitine palmitoyltransferase 1A and Adiponectin receptor type 2 and a tendency toward higher expression levels of the genes such as Fatty acid binding protein 1 and Long-chain acyl CoA dehydrogenase (Fig. 3). These responses were not observed in PPARα

knockout mice, indicating that 4-PAP activates PPARα *in vivo* (Fig. 3). Interestingly, similar to the results of our experiments using resveratrol (unpublished data), there was significantly 4-PAP-induced upregulation of SIRT1mRNA expression in wild-type, but not PPARα knockout mice (Fig. 3), indicating that PPARα-dependent upregulation of SIRT1 mRNA is attributable to SIRT1-activation by resveratrol *in vivo*.

Inhibition of PDE enhances the activation of PPARα by resveratrol

Finally, the inhibitory effect of PDEs on the activation of PPARα by resveratrol was examined using a luciferase reporter assay. BAECs were transiently transfected with the PPRE-luc reporter vector, the human PPARα expression vector GS-hPPARα, and pSV-β-gal as an internal control, and then incubated with varying concentrations of resveratrol, T4HS or 4-PAP for 24 h. At higher concentrations (from 10 μM to 40 μM), resveratrol had a more potent effect on the activation of PPARα than the others (Fig. 4A, left), on the other hand, resveratrol, T4HS and 4-PAP had the similar effect at lower concentrations (from 1.25 to 2.5 μM) (Fig. 4A, right). These results suggest that the 4′-hydroxyl group of resveratrol contributes to the activation of PPARα at up to 2.5 μM concentration, however, this 4′-hydroxyl group is not sufficient for the PPARα-activation at over 10 μM concentration.

A recent study reported that resveratrol inhibits PDE isozymes, PDE3 (IC_{50} = 10 μM) and PDE4 (IC_{50} = 14 μM), respectively [11]. It is therefore possible that the more potent effect of higher concentrations of resveratrol on the activation of PPARα is dependent on the inhibition of PDE, which will be contributed to the subsequent increase in intracellular cAMP levels. The activation of PPARα by 5 μM resveratrol, T4HS, or 4-PAP was enhanced by rolipram, a PDE4 inhibitor, or forskolin, an adenylate cyclase activator, both of which increase intracellular cAMP levels, although rolipram or forskolin alone could not activate PPARα (Fig. 4B). These results indicate that the activation of PPARα by resveratrol or its related compound is enhanced by cAMP. Thus, PPARα activation by resveratrol at an early point serves as a trigger to enhance the activation of PPARα in advance of the inhibition of PDE by resveratrol. Our PDE inhibition assay (Fig. 4C) revealed that resveratrol is a more potent inhibitor (IC_{50} = 19.0 μM) than T4HS (IC_{50} = 27.8 μM; $p = 0.00012$) and 4-PAP (IC_{50} = 26.5 μM; $p = 0.00022$), which explains the relatively greater effect of higher 10 μM concentration of resveratrol on the activation of PPARα (Fig. 4A). Zhao *et al.* recently reported that by different PDE4 assay using ^{3}H-cAMP, resveratrol is more potent inhibitor (IC_{50} = 14.0 μM) than pterostilbene (Fig. 1A) (IC_{50} = 27.0 μM) [29], which is similar to our PDE inhibitory data of T4HS and 4-PAP (Fig. 4C), indicating that the 4′-hydroxyl group of resveratrol partly contributes, but not sufficient, to inhibition of PDE.

This study investigated the molecular mechanisms involved in the activation of PPARα by resveratrol. An examination of the structure-activity relationships of resveratrol-related compounds revealed that the 4′-hydroxyl group of resveratrol is functionally important for the direct activation of PPARα (Fig. 1). This result was confirmed by a docking model simulation and a subsequent experiment using the crystal structure of the PPARα LBD (Fig. 2), as well as by an *in vivo* investigation of PPARα activation by resveratrol analog 4-PAP (Fig. 3). Remarkably, the induction of SIRT1 mRNA depends on the activation of PPARα by 4-PAP (Fig. 3) and resveratrol (unpublished data). Although direct activation of SIRT1 by resveratrol was unclear [9], [10], SIRT1 was reported to bind to PPARα and enhanced the transcriptional activity of PPARα with its co-activator PGC-1α and promotes fatty acid oxidation [30]. Therefore, there may be a feedforward activation of PPARα by resveratrol via activation of SIRT1.

Whereas the 4′-hydroxyl group of resveratrol directly contributes to PPARα activation, this 4′-hydroxyl group partly contributes to inhibition of PDE since the pattern of inhibition

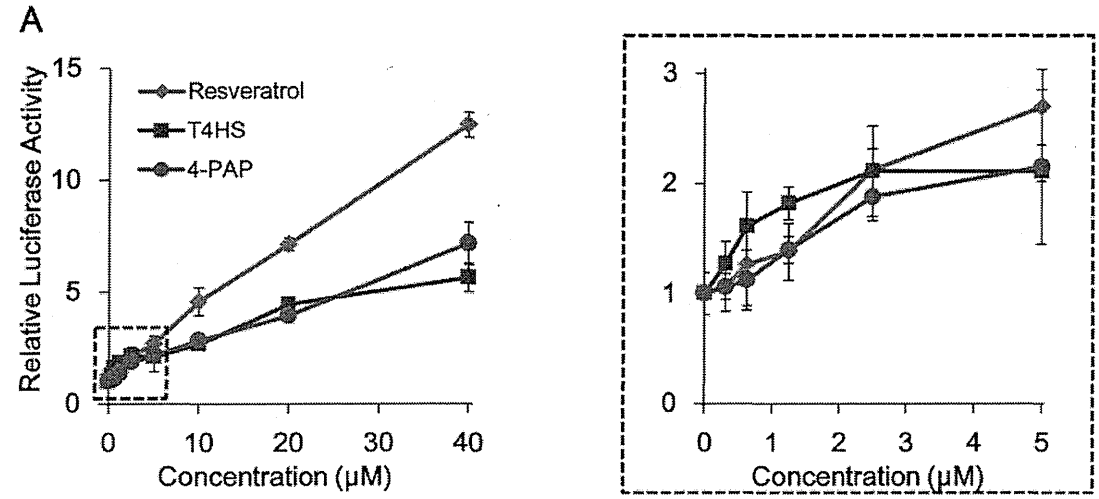

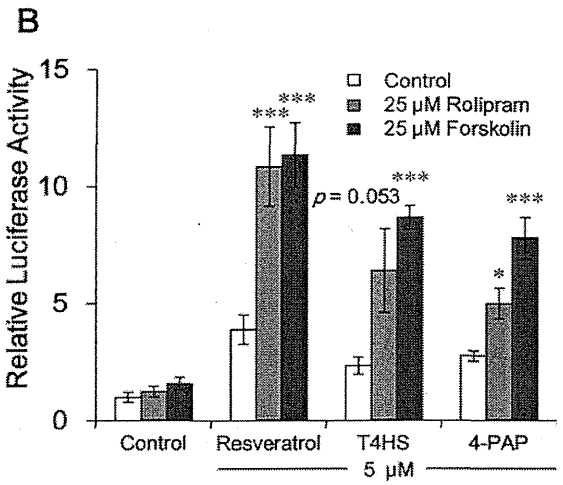

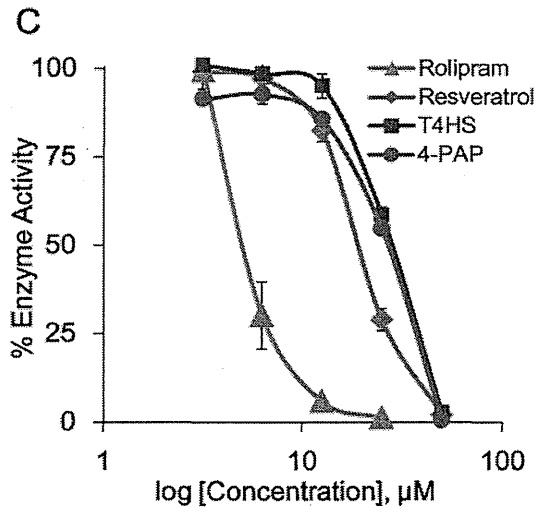

IC_{50} (μM)

Rolipram	5.3 ± 0.3	
Resveratrol	19.0 ± 0.4	***
T4HS	27.8 ± 0.7	*** ###
4-PAP	26.5 ± 0.1	*** ###

Fig 4. Takizawa et al.

Fig 4. Inhibition of PDE enhances the activation of PPARα by resveratrol, especially at higher doses. (A) The dose-dependent activation of PPARα by resveratrol, T4HS and 4-PAP in BAECs transiently transfected with PPRE-luc, GS-hPPARα, and pSV-β-gal. Following transfection, the cells were incubated for 24 h with resveratrol, T4HS or 4-PAP at the indicated concentrations. Data were normalized to the β-galactosidase standard and represent the mean ± SD of three independent wells of cells. The right graph corresponds to the lower area marked by a dashed rectangle in left graph. (B) cAMP-dependent enhancement of PPARα activation by resveratrol, T4HS or 4-PAP. BAECs transiently transfected with PPRE-luc, GS-hPPARα, and pSV-β-gal were incubated for 24 h with 5 μM compounds in the presence or absence of 25 μM rolipram, a PDE4 inhibitor, or 25 μM forskolin, an adenylate cyclase activator.

Luciferase data were normalized to the β-galactosidase standard and represent the mean ± SD of three independent wells. *$p < 0.05$, ***$p < 0.001$ (unpaired *t*-test) compared with control cells treated with the same compound. (C) The inhibition of PDE by resveratrol, T4HS, and rolipram. Data represent the mean ± SD of three independent wells of cells. Similar results were obtained by two additional experiments. The IC_{50} values are shown in the Table. ***$p < 0.001$ (unpaired *t*-test) compared with rolipram. ###$p < 0.001$ (unpaired *t*-test) compared with resveratrol. Similar results were obtained by two additional experiments in (A-C).

doi:10.1371/journal.pone.0120865.g004

differed between resveratrol, T4HS and 4-PAP (Fig. 4). Activation of PPARα by resveratrol was enhanced by its inhibition of PDE. This feedforward activation of PPARα by resveratrol may provide a reasonable explanation why long-term intake of resveratrol at concentrations lower than those used for *in vitro* assays induces the activation of PPARα *in vivo*. Fig. 5 shows

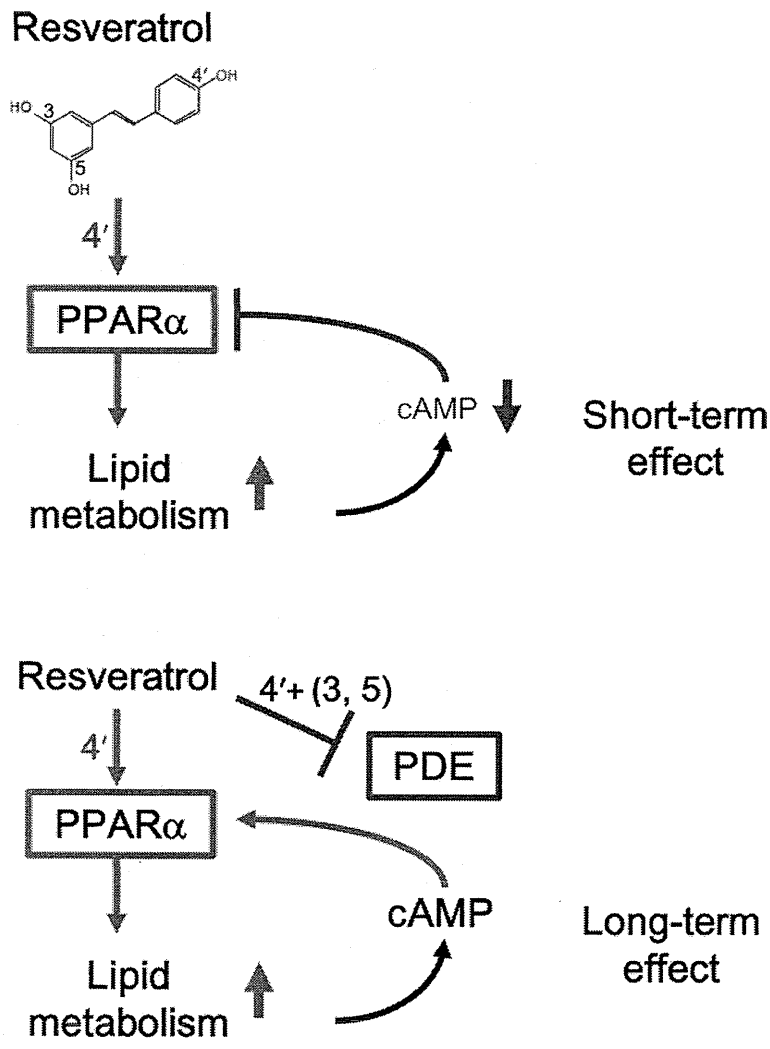

Fig 5. Takizawa et al.

Fig 5. Possible relationship among resveratrol, PPARα and PDE. These diagrams present our hypothesis about short- and long-term effects of resveratrol, as shown in the text.

doi:10.1371/journal.pone.0120865.g005

an ongoing hypothesis on long-term activation of PPARα by resveratrol *in vivo*. As a short-term effect, resveratrol activates PPARα, which induces PPARα responsive genes involved in lipid metabolism. Activation of lipid metabolism finally increases intracellular ratio of ATP/ADP, and will decrease intracellular cAMP levels, which may feedback control of PPARα–activation with a time lag. As a long-term effect, resveratrol inhibits PDE, which will enhance the PPARα-activation. At present, we do not have sufficient evidences for this hypothesis, especially feedback regulation of PPARα *in vivo*. Further study will need to evaluate this hypothesis.

Acknowledgments

We thank Drs. Shobu Namura and Takashi Nakazawa for helpful discussions and Ms. Haruka Takeuchi, Tomoko Tsukamoto, Naoko Anzai, Yukiko Kosuge, Emi Tamura, Ayako Takai for technical assistance.

Author Contributions

Conceived and designed the experiments: YT RN HI. Performed the experiments: YT RN HY HK HI. Analyzed the data: YT RN HY HK HI. Contributed reagents/materials/analysis tools: YT RN KF HY HK HI. Wrote the paper: YT RN HY HK HI.

References

1. Langcake P, Pryce RJ. The production of resveratrol by Vitis vinifera and other members of the Vitaceae as a response to infection or injury. Physiol Plant Pathol. 1976; 9: 77–86.
2. Jang M, Cai L, Udeani GO, Slowing KV, Thomas CF, Beecher CW, et al. Cancer chemopreventive activity of resveratrol, a natural product derived from grapes. Science. 1997; 275: 218–220. PMID: 8985016
3. Subbaramaiah K, Chung WJ, Michaluart P, Telang N, Tanabe T, Inoue H, et al. Resveratrol inhibits cyclooxygenase-2 transcription and activity in phorbol ester-treated human mammary epithelial cells. J Biol Chem. 1998; 273: 21875–21882. PMID: 9705326
4. Inoue H, Jiang XF, Katayama T, Osada S, Umesono K, Namura S. Brain protection by resveratrol and fenofibrate against stroke requires peroxisome proliferator-activated receptor α in mice. Neurosci Lett. 2003; 352: 203–206. PMID: 14625020
5. Howitz KT, Bitterman KJ, Cohen HY, Lamming DW, Lavu S, Wood JG, et al. Small molecule activators of sirtuins extend Saccharomyces cerevisiae lifespan. Nature. 2003; 425: 191–196. PMID: 12939617
6. Lastra CA, Villegas I. Resveratrol as an anti-inflammatory and anti-aging agent: mechanisms and clinical implications. Mol Nutr Food Res. 2005; 49: 405–430. PMID: 15832402
7. Baur JA, Sinclair DA. Therapeutic potential of resveratrol: the in vivo evidence. Nat Rev Drug Discov. 2006; 5: 493–506. PMID: 16732220
8. McCay CM, Crowell MF, Maynard LA. The effect of retarded growth upon the length of life span and upon the ultimate body size. J Nutr. 1935; 10: 63–79.
9. Kaeberlein M, McDonagh T, Heltweg B, Hixon J, Westman EA, Caldwell SD, et al. Substrate-specific activation of sirtuins by resveratrol. J Biol Chem. 2005; 280:17038–17045. PMID: 15684413
10. Pacholec M, Bleasdale JE, Chrunyk B, Cunningham D, Flynn D, Garofalo RS, et al. SRT1720, SRT2183, SRT1460, and resveratrol are not direct activators of SIRT1. J Biol Chem. 2010; 285: 8340–8351. doi: 10.1074/jbc.M109.088682 PMID: 20061378
11. Park SJ. Resveratrol ameliorates aging-related metabolic phenotypes by inhibiting cAMP phosphodiesterases. Cell. 2012; 148: 421–433. doi: 10.1016/j.cell.2012.01.017 PMID: 22304913
12. Nakata R, Takahashi S, Inoue H. Recent advances in the study on resveratrol. Biol Pharm Bull. 2012; 35: 273–270. PMID: 22382311
13. Tsukamoto T, Nakata R, Tamura E, Kosuge Y, Kariya A, Katsukawa M, et al. Vaticanol C, a resveratrol tetramer, activates PPARα and PPARβ/δ in vitro and in vivo. Nutr Metab. 2010; 7: 46.
14. Corton JC, Apte U, Anderson SP, Limaye P, Yoon L, Latendresse J, et al. Mimetics of caloric restriction include agonists of lipid-activated nuclear receptors. J Biol Chem. 2004; 279: 46204–46212. PMID: 15302862

15. Mangelsdorf DJ, Thummel C, Beato M, Herrlich P, Schütz G, Umesono K, et al. The nuclear receptor superfamily: the second decade. Cell. 1995; 83: 835–839. PMID: 8521507

16. Michalik L, Auwerx J, Berger JP, Chatterjee VK, Glass CK, Gonzalez FJ, et al. International Union of Pharmacology. LXI. Peroxisome proliferator-activated receptors. Pharmacol Rev. 2006; 58: 726–741. PMID: 17132851

17. Xu HE, Lambert MH, Montana VG, Parks DJ, Blanchard SG, Brown PJ, et al. Molecular recognition of fatty acids by peroxisome proliferator-activated receptors. Mol Cell. 1999; 3: 397–403. PMID: 10198642

18. Forman BM, Tontonoz P, Chen J, Brun RP, Spiegelman BM, Evans RM. 15-Deoxy-delta 12,14-prostaglandin J_2 is a ligand for the adipocyte determination factor PPARγ. Cell. 1995; 83: 803–812. PMID: 8521497

19. Kliewer SA, Lenhard JM, Willson TM, Patel I, Morris DC, Lehmann JM. A prostaglandin J_2 metabolite binds peroxisome proliferator-activated receptor gamma and promotes adipocyte differentiation. Cell. 1995; 83: 813–819. PMID: 8521498

20. Inoue H, Tanabe T, Umesono K. Feedback control of cyclooxygenase-2 expression through PPARγ. J Biol Chem. 2000; 275: 28028–28032. PMID: 10827178

21. Inoue H, Taba Y, Miwa Y, Yokota C, Miyagi M, Sasaguri T. Transcriptional and Posttranscriptional Regulation of Cyclooxygenase-2 Expression by Fluid Shear Stress in Vascular Endothelial Cells. Arterioscler Thromb Vasc Biol. 2002; 22: 1415–1420. PMID: 12231559

22. Thakkar K, Geahlen RL, Cushman M. Synthesis and protein-tyrosine kinase inhibitory activity of polyhydroxylated stilbene analogues of piceatannol. J Med Chem. 1993; 36: 2950–2955. PMID: 8411012

23. Hotta M, Nakata R, Katsukawa M, Hori K, Takahashi S, Inoue H. Carvacrol, a component of thyme oil, activates PPARα and γ and suppresses COX-2 expression. J Lipid Res. 2010; 51: 132–139. doi: 10.1194/jlr.M900255-JLR200 PMID: 19578162

24. Jones G, Willett P, Glen RC, Leach AR, Taylor R. Development and validation of a genetic algorithm for flexible docking. J Mol Biol. 1997; 267: 727–748. PMID: 9126849

25. Kuhn B, Kollman PA. Binding of a diverse set of ligands to avidin and streptavidin: an accurate quantitative prediction of their relative affinities by a combination of molecular mechanics and continuum solvent models. J Med Chem. 2000; 43: 3786–3791. PMID: 11020294

26. Kleppisch T. Phosphodiesterases in the central nervous system. Handb Exp Pharmacol. 2009; 191: 71–92. doi: 10.1007/978-3-540-68964-5_5 PMID: 19089326

27. Xu HE, Lambert MH, Montana VG, Plunket KD, Moore LB, Collins JL, et al. Structural determinants of ligand binding selectivity between the peroxisome proliferator activated receptors. Proc Natl Acad Sci USA. 2001; 98: 13919–13924. PMID: 11698662

28. Calleri E, Pochetti G, Dossou KS, Laghezza A, Montanari R, Capelli D, et al. Resveratrol and its metabolites bind to PPARs. ChemBioChem. 2014; 15: 1154–1160. doi: 10.1002/cbic.201300754 PMID: 24796862

29. Zhao P, Chen SK, Cai YH, Lu X, Li Z, Cheng YK, et al. The molecular basis for the inhibition of phosphodiesterase-4D by three natural resveratrol analogs. Isolation, molecular docking, molecular dynamics simulations, binding free energy, and bioassay. Biochim Biophys Acta. 2013; 1834: 2089–2096. doi: 10.1016/j.bbapap.2013.07.004 PMID: 23871879

30. Purushotham A, Schug TT, Xu Q, Surapureddi S, Guo X, Li X. Hepatocyte-specific deletion of SIRT1 alters fatty acid metabolism and results in hepatic steatosis and inflammation. Cell Metab. 2009; 9: 327–338. doi: 10.1016/j.cmet.2009.02.006 PMID: 19356714

ChemComm

COMMUNICATION

View Article Online
View Journal | View Issue

Cite this: *Chem. Commun.*, 2015, 51, 8311

Received 17th March 2015,
Accepted 8th April 2015

DOI: 10.1039/c5cc02236c

www.rsc.org/chemcomm

Solubilisation of a 2,2-diphenyl-1-picrylhydrazyl radical in water by β-cyclodextrin to evaluate the radical-scavenging activity of antioxidants in aqueous media†

Ikuo Nakanishi,*[a] Kei Ohkubo,[bc] Kohei Imai,[d] Masato Kamibayashi,[e] Yasuo Yoshihashi,[f] Ken-ichiro Matsumoto,[a] Kiyoshi Fukuhara,[d] Katsuhide Terada,[f] Shinobu Itoh,[b] Toshihiko Ozawa[g] and Shunichi Fukuzumi*[bchi]

A 2,2-diphenyl-1-picrylhydrazyl radical (DPPH•) was successfully solubilised in water by β-cyclodextrin (β-CD). DPPH•/β-CD thus obtained was demonstrated to be a powerful tool to evaluate the antioxidative activity of water-soluble antioxidants, such as ascorbate and Trolox, in aqueous buffer solutions.

A relatively stable radical, 2,2-diphenyl-1-picrylhydrazyl (DPPH•) (Scheme 1), is frequently used as a reactivity model of reactive oxygen species (ROS) to evaluate the radical-scavenging activity of antioxidants.[1–6] DPPH• shows a characteristic absorption band at around 520 nm, which disappears upon addition of compounds with radical-scavenging activity. However, alcoholic cosolvents, such as methanol and ethanol, are required to use DPPH• in aqueous systems due to its little solubility in water.[7–9] In such a case, concentrated buffer solutions cannot be used to control the pH of the reaction systems because buffer salts are precipitated in the alcoholic reaction media. Cyclodextrins (CDs) are cyclic oligosaccharides that have a hydrophobic internal cavity and a hydrophilic external surface. Thus, CDs form inclusion complexes with a wide range of hydrophobic molecules and solubilise them in water.[10,11] We report herein the solubilisation of DPPH• in water using β-cyclodextrin (β-CD: Scheme 1), which consists of 7 glucopyranoside units. The scavenging reaction of β-CD-solubilised DPPH• (DPPH•/β-CD) by water-soluble antioxidants in phosphate buffer solution (0.1 M, pH 7.4) demonstrated that DPPH•/β-CD would be a powerful tool to evaluate the anti-oxidative activity in aqueous media without alcoholic cosolvents.

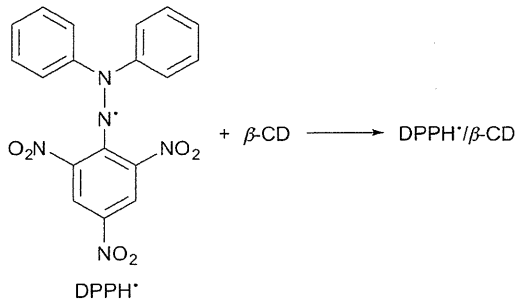

Scheme 1 Incorporation of DPPH• into β-cyclodextrin (β-CD).

15 mL of boiling water (Milli-Q) or a phosphate buffer solution (0.1 M, pH 7.4) was added to the mixture containing DPPH• (0.23 mmol) and β-CD (0.35 mmol), and the suspension was cooled to room temperature. The filtration of the suspension using a membrane filter (pore size: 0.22 μm) gave a deep violet solution. This solution showed an absorption band at 527 nm, which is diagnostic of DPPH• (Fig. 1). Thus, DPPH• could be solubilised in water by β-CD. A significant red shift of the band due to DPPH•/β-CD as compared to those of free DPPH• in *n*-hexane (509 nm), MeOH (516 nm), EtOH (517 nm) and aceto-nitrile (519 nm) suggests that the >N–N•– moiety of DPPH• may exist outside of the β-CD cavity and strongly interact with water. The concentration of DPPH• was estimated to be 5.9×10^{-5} M by using the ε value of 11 000 M^{-1} cm^{-1} determined for DPPH• in a 1 : 1 ethanol–buffer solution.[9] When β-CD was replaced by α- or γ-CD, which consists of 6 or 8 glucopyranoside units and thus has a smaller or bigger hydrophobic cavity than β-CD,

[a] *Radio-Redox-Response Research Team, Advanced Particle Radiation Biology Research Program, Research Center for Charged Particle Therapy, National Institute of Radiological Sciences (NIRS), Inage-ku, Chiba 263-8555, Japan. E-mail: nakanis@nirs.go.jp; Fax: +81-43-255-6819; Tel: +81-43-206-3131*
[b] *Department of Material and Life Science, Graduate School of Engineering, Osaka University, Suita, Osaka 565-0871, Japan*
[c] *ALCA and SENTAN, Japan Science and Technology Agency (JST), Suita, Osaka 565-0871, Japan*
[d] *School of Pharmacy, Showa University, Shinagawa-ku, Tokyo 142-8555, Japan*
[e] *Pharmaceutical Manufacturing Chemistry, Kyoto Pharmaceutical University, Kyoto 607-8414, Japan*
[f] *Department of Pharmaceutics, Faculty of Pharmaceutical Sciences, Toho University, Funabashi, Chiba 274-8510, Japan*
[g] *Division of Oxidative Stress Research, Showa Pharmaceutical University, Machida, Tokyo 194-8543, Japan*
[h] *Department of Bioinspired Science, Ewha Womans University, Seoul 120-750, Korea*
[i] *Faculty of Science and Technology, Meijo University, Shiogamaguchi, Tempaku, Nagoya, Aichi 468-8502, Japan*

† Electronic supplementary information (ESI) available: Experimental details and EPR spectra at room temperature (Fig. S1). See DOI: 10.1039/c5cc02236c